

Resolving the Geometry/Charge Puzzle of the c(2x2)-Cl Cu(100) Electrode

Kathleen Schwarz,^{*,†} Mitchell C. Groenenboom,[†] Thomas P. Moffat,[†]

Ravishankar Sundararaman,[‡] and John Vinson[†]

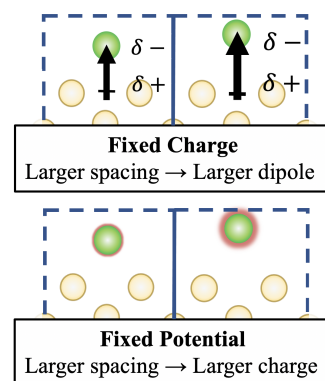
[†]Material Measurement Laboratory, National Institute of Standards and Technology, 100 Bureau Dr., Gaithersburg, Maryland 20899, United States

[‡]Department of Materials Science and Engineering, Rensselaer Polytechnic Institute, 110 8th St., Troy, New York 12180, United States

Received December 29, 2020; E-mail: kas4@nist.gov

Abstract:

Potential-induced changes in charge and surface structure are significant drivers of the reactivity of electrochemical interfaces, but are frequently difficult to decouple from the effects of surface solvation. Here, we consider the Cu(100) surface with a c(2x2)-Cl adlayer, a model surface with multiple geometry measurements under both ultrahigh vacuum and electrochemical conditions. Under aqueous electrochemical conditions, the measured Cu-Cl interplanar separation (d_{Cu-Cl}) increases by at least 0.3 Å relative to that under ultrahigh vacuum conditions. This large geometry change is unexpected for a hydrophobic surface and it requires invoking a negative charge on the Cl-covered surface much greater than expected from the work function and our capacitance measurements. To resolve this inconsistency we employ *ab initio* calculations and find that the Cu-Cl separation increases with charging at a rate of 0.7 Å/e⁻ per Cl atom. The larger Cu-Cl bond distance increases the surface dipole and therefore, the work function of the interface, contributing to the negative charge under fixed potential electrochemical conditions. Interactions with water are not needed to explain either the large charge or large Cu-Cl interplanar spacing of this surface under electrochemical conditions.



The relationship between the work function of a clean surface measured in vacuum and the potential of zero charge for that same surface in electrolyte serves as a bridge between surface science and electrochemistry.¹⁻³ The work function of a surface corresponds to its potential of zero charge (referenced to the absolute electrode potential of 4.44 V vs. SHE, the Standard Hydrogen Electrode³) *only* if it acts as a perfectly non-interacting electrode. No electrode is expected to be perfectly non-interacting. Instead, the surface frequently interacts with the electrolyte through charge transfer and orientation of the solvent. These interactions cause deviations between the measured potential of zero charge (PZC) and the value extrapolated from the work function.

Here, we consider two surfaces, Cu(100) and that surface with a c(2x2) Cl adlayer, that have been extensively characterized under both ultrahigh vacuum⁴⁻¹⁰ and electrochemical¹¹⁻²¹ conditions. For these surfaces, Figure 1 depicts the known experimental values for the work function and potential of zero charge.

Under ultra-high vacuum (UHV) conditions, Cl forms a well-defined c(2x2) adlayer on the Cu(100) surface and increases its work function by 1.1 eV.⁸ This work function increase is due to the increase in the magnitude of the surface dipole, and occurs upon Cl binding to many other metal surfaces as well.^{22,23}

The Cl adlayer changes significantly from UHV to electrochemical conditions (i.e., in aqueous solution at potentials near 0 V vs. SHE): the electrode is hypothesized to be highly negatively charged,²¹ the Cu-Cl interlayer separation (d_{Cu-Cl} , the interplanar distance from the Cl to the first-layer Cu atoms) increases by 0.3 Å (Figure 2), and the subtle

buckling of the second layer of Cu, Δ_2 (i.e., the difference in interplanar height between the two Cu atoms in the unit cell in the second layer of Cu, see schematic in Figure 2) may reverse direction or attenuate.^{10,13,15,17,18,21}

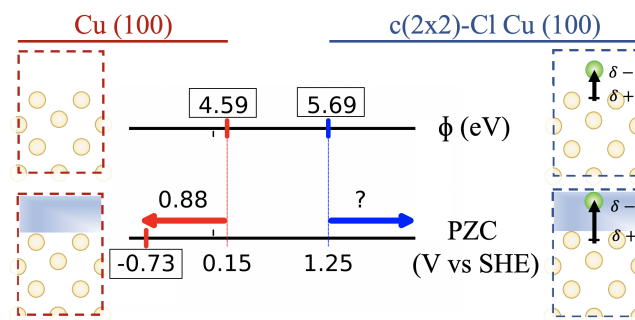


Figure 1. Schematics depict the Cu(100) surface (left) and the c(2x2)-Cl Cu(100) surface (right) under vacuum and under electrochemical conditions, respectively, with copper atoms in orange and Cl atoms in green. Experimental work functions (Φ) and their extrapolated PZC's (Work function minus 4.44 V vs SHE) of Cu(100) (red, left side)⁹ and Cu(100) with a c(2x2) Cl adlayer⁸ (blue, right side), with experimental Cu(100) PZC in aqueous, noninteracting media.¹⁶

In contrast, in the case of Cu(100) *without* Cl, the planar separation between the first two Cu layers does not change appreciably between UHV and electrochemical conditions, the electrode is positively charged, and the surface does not buckle.^{13,15} When exposed to aqueous solution, the Cl-covered copper surface only weakly interacts with water. Likewise, under UHV conditions water does not stick to the Cl-covered Cu(100) surface at room temperature, and

the presence of water does not change the Cu-Cl interlayer separation, within the experimental uncertainty.⁶ Density functional theory calculations support this, finding that a bilayer of water on this surface only weakly binds through van der Waals interactions.⁶ Furthermore, surface-enhanced infrared absorption spectroscopy (SEIRAS) measurements of chloride adsorption on a polycrystalline Cu thin film in acid medium indicate an increase in non-hydrogen bonded interfacial water, suggestive of halide-induced hydrophobicity.²⁴ The experimentally estimated capacitance of this surface is also quite low,¹⁴ similar to other systems with hydrophobic adsorbates such as CO (11 $\mu\text{F}/\text{cm}^2$ for Pt(111)^{25,26}). The Cl-covered surface thus appears to only weakly interact with water, in contrast to halide-free Cu(100),^{4,5,27,28} Cu(110) and Cu(111).²⁹ Surfaces that interact weakly with water would not be expected to exhibit large geometry changes in moving from vacuum to aqueous conditions.

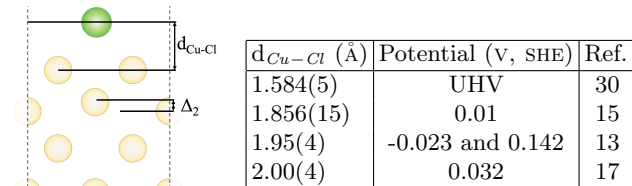


Figure 2. Experimental Cu-Cl interlayer separation $d_{\text{Cu-Cl}}$ from X-ray diffraction for ultra high vacuum and electrochemical conditions (aqueous solutions of 10 mmol/L HCl), with uncertainties given in parentheses. Schematic depicts $d_{\text{Cu-Cl}}$ and Δ_2 , the buckling of second Cu layer.

Here, we resolve this seeming contradiction between the chloride-covered surface’s apparently weak solvent interaction,^{6,24} and the significant Cu-Cl interlayer separation increase and large negative interfacial charge under electrochemical conditions.^{10,13,15,17,18,21} We find that, even though the adsorption of halide changes the surface’s work function by approximately 1 V, the potential difference between the PZC of the Cu and the extrapolated “virtual” or “fictitious”^{*} PZC of the charged Cl-covered electrodes is approximately 3 V. The difference in the PZC of Cu(100), and the virtual PZC of the Cu(100) with the ordered Cl adlayer, can be divided into three roughly 1 V contributions:

1. the downward shift in PZC of the bare Cu surface due to interaction with water^{27,28}
2. the work function difference between the Cu and Cl-covered surfaces in vacuum⁸
3. the work function increase of the Cl-covered surface due to increased Cu-Cl interlayer spacing under the imposed electrochemical conditions, caused in turn by the negative electrode charge.

The first two contributions above are already known from experiments and first-principles calculations, as we discuss briefly below. Consequently, we focus on the previously unknown third contribution, combining independent evidence

^{*}The PZC of the Cl-covered electrodes is not experimentally accessible because the Cu surface begins dissolving at potentials significantly lower than it. Here we evaluate a fictitious PZC, the “virtual” PZC based on the geometry of the experimentally accessible, negatively charged Cl-covered electrode, for the purposes of decomposing the contributions to the surface charge of the experimentally accessible surface. The value of the virtual PZC depends on potential, and as the potential increases toward the PZC, the charge and the Cu-Cl interlayer spacing must eventually decrease to approximately the vacuum values.

from first-principles calculations and experiment. Our *ab initio* calculations predict a large charge on the electrode ($\approx 0.4 e^-$ per Cl atom) under the relevant electrochemical conditions (aqueous solution at potentials near 0 V vs SHE), and find that $d_{\text{Cu-Cl}}$ increases dramatically with increasing charge ($\approx 0.7 \text{ \AA}/e$ per Cl atom). We show that the work function of the surface increases as the electrode geometry changes with increasing negative charge. This increases the virtual PZC, further driving up the negative charge. Independently, we find a low experimental capacitance, implying a large potential difference from the virtual PZC for the calculated surface charge.

We perform *ab initio* calculations and experimental capacitance measurements of the Cu(100) surface with a $c(2 \times 2)$ adlayer of Cl. All calculations are performed with the Perdew–Burke–Ernzerhof (PBE)³¹ exchange-correlation potential unless identified as Heyd–Scuseria–Ernzerhof (HSE).³² We model this surface with 20 Cu atoms (10 layers) and two Cl atoms (top and bottom of the slab), and we use lattice vectors from optimization of bulk copper using HSE, 6.850 Bohr. All calculations are periodic, using a plane wave cutoff of 120 Ry, $8 \times 8 \times 1$ k-point sampling, and Pseudo-Dojo pseudopotentials with nonlinear core-corrections removed for HSE.³³ Effective screening medium method (ESM) calculations are carried out with QUANTUM ESPRESSO 6.5,³⁴ using a box height of 60 Bohr.[†] Vacuum or metal boundary conditions are used in the ESM for neutral or charged systems, respectively. ESM calculations with HSE are also calculated with QUANTUM ESPRESSO, using the Adaptively Compressed Exchange method³⁵ modified to perform single-precision numerics.³⁶ The exact-exchange operator was calculated on a $4 \times 4 \times 1$ k-point grid. Bader charges were evaluated using the Yu-Trinkle method implemented in Critic2.^{37–41} All other calculations are performed in JDFTx,⁴² using solvation models (CANDLE,⁴³ LinearPCM⁴⁴) with 1 mol/L electrolyte in water to charge the cell (See Ref. 45 for an overview of these methods), Coulombic truncation, and a box height of 70 Bohr.

The Cu(100) crystal was prepared by electropolishing in neat phosphoric acid followed by extensive rinsing with 18 M Ω -cm water. The crystal was then transferred to another electrochemical cell containing 0.1 mol/L H_2SO_4 with 0.001 mol/L Cl^- that was deaerated before and during the experiment with Ar. The specimen was immersed under potential control and poised at 0.042 V vs. SHE. Voltammetry was performed at a variety of sweep rates ranging from 0.1 to 1.0 V/s. The capacitance associated with the Cu(100) surface with the saturated $c(2 \times 2)$ Cl adlayer was determined from the scan rate dependence of the voltammetric current at 0.032 V vs. SHE.

The bare Cu(100) has a PZC that is 0.88 V less than that predicted solely from the work function,¹⁶ as shown in Figure 1. This nearly 1 V overestimate of the work-function derived PZC is similar to that found for platinum, silver, and gold. A number of attempts have been made to identify the interactions of real electrodes that cause these differences. Early work on single-crystal metal surfaces such as platinum and silver in aqueous electrolyte attributed differences between the work function and the PZC to the reorientation of water molecules near the interface.⁴⁷ Recent *ab ini-*

[†]Note: Certain commercial software are identified in this paper to foster understanding. Such identification does not imply recommendation or endorsement by the National Institute of Standards and Technology, nor does it imply that the software identified is necessarily the best available for the purpose.

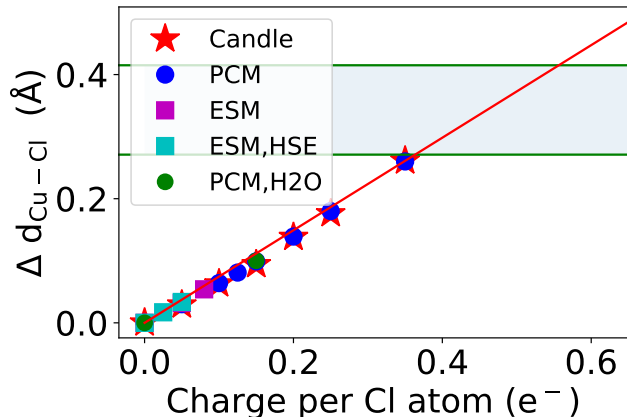


Figure 3. Change in d_{Cu-Cl} with charge per Cl atom from *ab initio* calculations. Surfaces were charged with continuum solvation models with ionic screening (Candle,⁴³ PCM⁴⁴) and ESM.⁴⁶ Green horizontal lines indicate the bounds of the experimental d_{Cu-Cl} change (from top to bottom, Ref. 15,17), relative to the vacuum value.³⁰ The red line is the extrapolation from the highest charge PCM result.

tio molecular dynamics calculations have suggested that for a set of these metals, the orientation contribution is minor, and rather, the difference is primarily due to electron transfer from the oxygen atom in water to the metal surface.²⁷ It is reasonable to anticipate that the Cu(100) surface has significant charge transfer to the metal from the electrons on the oxygen in water, similar to the metal surfaces considered by Ref. 27. Regardless of whether the PZC shifts because of water orientation or electronic effects, this shift is evident from the work function shift upon water adsorption on Cu(100). Experiments find a work function shift of -0.7 eV⁴ to -0.9 eV⁵ upon adsorption of water. A similar shift (-1.1 eV) has also been found with density functional theory (DFT).⁴⁸ These downward work function shifts due to interaction with water account for the 0.88 V downward shift of the Cu(100) PZC relative to that expected from the work function in the absence of water.

For the Cu surface with $c(2 \times 2)$ -Cl, the work function is (5.69 ± 0.1) eV^{8,9} ‡. This value is 1.1 eV higher than the work function of the Cu(100) surface due to the larger surface dipole induced by the Cl adlayer.

The work function of the halide-covered surface corresponds to a PZC of 1.25 V vs SHE. However, experiments and DFT calculations²¹ around 0 V vs SHE suggest that the electrode with $c(2 \times 2)$ Cl is even more negatively charged than one would expect given that PZC and a typical value for the capacitance of an adsorbate-covered metal surface. We investigate the charge on the electrode with *ab initio* methods.

Applying a negative charge to the electrode, we find the increase in Cu-Cl interlayer spacing relative to the vacuum geometry. Figure 3 shows a linear relationship between the electrode charge and d_{Cu-Cl} for DFT calculations in the d_{Cu-Cl} range of interest as defined from the literature values from single-crystal X-ray diffraction (SXRD) studies. We find that the d_{Cu-Cl} changes with charge identically for both continuum solvation model charging (LinearPCM and Candle) and that with the countercharge on a charged wall,

‡Ref. 9 reports this quantity as (1.1 ± 0.1) eV larger than Cu(100) work function, which was determined to be (4.60 ± 0.05) eV by Ref. 8, and (4.59 ± 0.03) eV by Ref. 9.

using the effective screening medium approach.⁴⁹ Additionally, we find the same linear relationship, *regardless* of the method of calculation. We compare PBE DFT with HSE, and the exact exchange does not change the slope of this line. However, the magnitude of charging for the HSE and ESM cases is limited compared to that of JDFTx because of convergence challenges in QUANTUM ESPRESSO. The experimental increases in d_{Cu-Cl} are reported by others to be between 0.27 Å and 0.42 Å (Figure 2). Extrapolating from the highest charge PCM result, these d_{Cu-Cl} correspond to a predicted negative charge on the electrode of 0.36 e⁻ to 0.56 e⁻ per Cl atom. We note though that the linear relationship observed for all calculation methods will break down in the regime where the bond breaks.

Others^{15,21} have also performed negatively charged DFT calculations using one Ca²⁺ counterion per every two Cl atoms (nominally 1 e⁻ per Cl atom). However, they do not predict the charge on the electrode at the potentials of interest, beyond identifying it as negative, or they work from “the assumption that chloride anions retain almost their full charge in the electrochemical environment upon adsorption on copper”.¹⁷

To determine whether water interacts with the Cu-Cl and modifies the Cu-Cl polarizability or work function, we also charge the slab using continuum solvation and a single explicit water molecule, using DFT. We find that under neutral conditions, the water molecule interacts with the Cl in its 4-fold hollow position in the $c(2 \times 2)$ lattice, and does not cause the d_{Cu-Cl} to noticeably increase. This result agrees with findings from previous DFT studies of the neutral surface that have found that a bilayer of water does not significantly interact with the surface beyond van der Waals interactions,⁶ and that water only slightly increases d_{Cu-Cl} (by 0.03 Å).¹⁵ We find here that the d_{Cu-Cl} in the presence of water does not noticeably deviate from that of the continuum-only case when the charge is increased to 0.15 e⁻ per Cl atom. We note that at higher charges, the single water DFT model begins behaving both unphysically and differently from experiment, with the Cl moving from the 4-fold hollow, the charge on the downward-pointing H increasing, and that O-H bond length increasing (See structure in Supporting Information). This could be due to a semilocal DFT self-interaction error, but verification requires an HSE calculation at a charge beyond what we can currently converge.

To explain how the charge on the electrode increases to reach the large value we predict at potentials near 0 V vs SHE, we need to find the capacitance of the interface, and the potential difference between the potential of interest and the potential of zero charge. Sources of this large charge include the following possibilities:

- a constant, high value of the capacitance
- a capacitance that increases with potential near the PZC
- a virtual PZC much higher than work function predictions from the vacuum structure

Potentials at the PZC estimated from the work function (1.25 V vs SHE) and above it are not experimentally accessible, because the Cu(100) surface dissolves at potentials above 0.1 V vs the standard hydrogen electrode.^{13–15,17,18} However, the differential capacitance of the Cu(100) surface

with the $c(2 \times 2)$ -Cl adlayer at lower potentials is easily measurable.

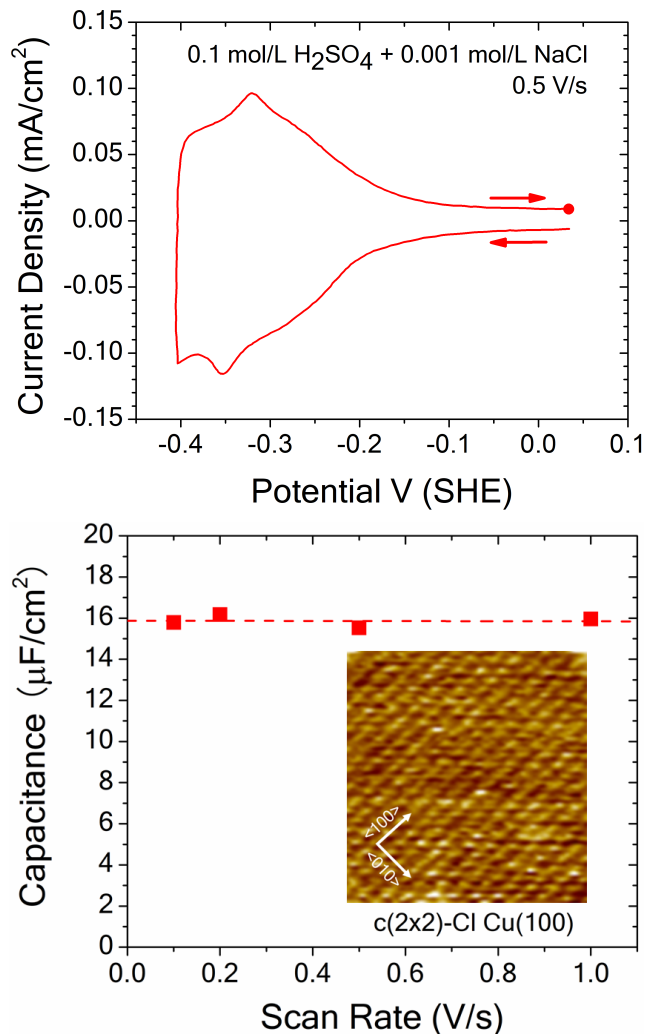


Figure 4. The capacitance associated with the saturated $c(2 \times 2)$ -Cl- Cu(100) was determined from the scan rate dependence of the voltammetric current at 0.032 V vs SHE. (a) plots the current density for the scan at 0.5 V/s. The dashed line in (b) is the average differential capacitance from the positive and negative scans from 0.1 V/s to 1.0 V/s, yielding a value close to $16 \mu\text{F}/\text{cm}^2$ independent of scan rate. The inset in (b) is a scanning tunneling microscope image of the surface at 0.0 V vs SHE depicting the $c(2 \times 2)$ adlattice of the Cl.

We experimentally measure the capacitance of the Cu(100) with $c(2 \times 2)$ -Cl to be $16 \mu\text{F}/\text{cm}^2$ at 0.032 V vs SHE, as shown in Figure 4 (Reference 14 also estimates from experiment a low double layer capacitance for this system). For this surface, a capacitance of $16 \mu\text{F}/\text{cm}^2$ corresponds to a change in charge of $0.13 e^-$ per Cl atom over 1 V (or equivalently $0.16 e^-$ per Cl atom over 1.25 V). $0.16 e^-$ is considerably less than the minimum estimated $0.36 e^-$ expected from the change in $d_{\text{Cu-Cl}}$. If this capacitance is constant at all potentials between 0 V vs. SHE and the PZC, we expect the virtual potential of zero charge to be 2.7 V vs. SHE.

We have seen that for other adsorbates (CO on Pt, Ref 25,26), the capacitance contributions of the region between the electrolyte and adsorbate dominate the capacitance, suggesting that the same may be true for this system as well. These calculations on similar systems suggest that the capacitance near the PZC would not be dramatically higher

than the $16 \mu\text{F}/\text{cm}^2$ measured far from the PZC. However, future computational work is needed to accurately determine the capacitance at the PZC of this surface.

Lastly, we evaluate the change in the computed work function with increasing Cu-Cl distance, $d_{\text{Cl-Cu}}$. Specifically, we perform a fixed-geometry, neutral, vacuum calculation to evaluate the work function of the slab geometry taken from a charged, solvated⁴⁴ calculation. These results are shown in Figure 5, labeled “PCM”. We then find the work function from the equilibrium geometry of a neutral, vacuum calculation, perturbed by incrementally displacing the Cl atoms from the slab. This is shown in the dataset labeled “Stretch”. Both geometries yield nearly identical results, and the work function increases linearly with increasing Cu-Cl interlayer separation.

We also compare the PBE results with those from HSE. The experimental work function agrees slightly better with the HSE result versus the PBE one. We also note that the slopes of the best fit lines for PBE and HSE differ. Due to the expense of the exact exchange used in hybrid functionals including HSE, DFT studies of copper with halides^{6,50-52} generally rely on semilocal functionals such as PBE as being sufficiently correct. However, the use of semilocal functionals can lead to significant errors at interfaces with adsorbates. In fact, surfaces have some of the most well-documented *ab initio* method failures, including self-interaction errors (the Pt-CO problem),⁵³ overly distributed electron-densities of dielectric surfaces,⁵⁴ and lack of van der Waals interactions.⁵⁵ Additionally, halides specifically have been found to have self-interaction errors.⁵⁶ Thus, we use the slope of the best fit line for the HSE data to give a predicted virtual PZC estimate of 2.3 V to 2.9 V vs SHE corresponding to the range of experimental $d_{\text{Cu-Cl}}$ (see Figure 2) under electrochemical conditions.

To understand the work function changes and the source of the difference between the HSE and PBE work function results, we assume a simple model of the surface dipole. We consider the dipole change due to the outward movement of the Cl, using the Bader charge for the charge of the Cl atom. When the Cl atom with charge q is moved normal to the surface, we expect a change in potential per unit displacement $dV/dx = q/(2\epsilon_0 A)$, where A is the area of the surface unit cell and ϵ_0 is the vacuum dielectric. The Bader charge on the Cl atoms is 0.49 (0.53) in PBE (HSE) for the vacuum geometry, which corresponds to a slope of 3.36 (3.64) V/Å in good agreement with the observed slope in Fig. 5 of 3.31 (3.92) V/Å. Therefore the linear change in work function is predominantly from the change in surface dipole layer as defined by the increase in $d_{\text{Cu-Cl}}$. Additionally, the work function difference between HSE and PBE is due to the differences in their charge distribution at the surface.

In summary, the Cl adsorption as a $c(2 \times 2)$ adlayer on the Cu(100) surface dramatically changes the charge on the electrode relative to that of the Cl-free case, and the behavior of this hydrophobic Cl-covered surface is not driven by interactions with water. In the case of the Cl-free electrode, the PZC is approximately 1 V *below* that expected from the Cu(100) work function, due to the interactions with water. In contrast, the Cu-Cl interlayer spacing increases as the negative charge on the electrode increases, driving up the virtual PZC by approximately 1 V *above* that predicted by the work function of the Cu(100) with $c(2 \times 2)$ Cl.

We extrapolate to find the virtual PZC of the $c(2 \times 2)$ -Cl Cu(100) surface using two different sets of assumptions. In

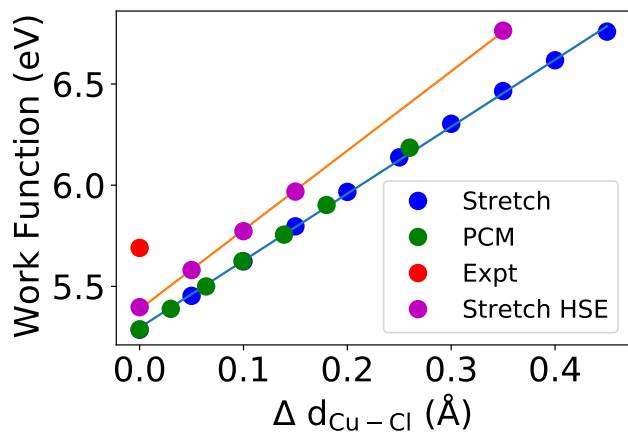


Figure 5. Work function as a function of d_{Cu-Cl} difference from neutral vacuum geometry, for geometries with the Cl displaced from vacuum position (Stretch, Stretch HSE) and geometries from calculations charged with PCM (PCM). Best fit lines for PCM and Stretch HSE are shown. Experiment from Ref 8,9.

one, we assume a constant capacitance, using the experimental value for the differential capacitance ($16 \mu\text{F}/\text{cm}^2$), and the total estimated charge ($0.36 e^-$ to $0.56 e^-$ per Cl atom). From this, we find a virtual PZC of 2.7 V to 4.3 V vs SHE. We note that this estimate is significantly limited by the assumption of constant capacitance. In the other, we take the experimental Cu-Cl interlayer spacing, and consider the work function increase with increasing d_{Cu-Cl} with HSE, estimating a virtual PZC that is 2.3 V to 2.9 V vs SHE. Considering that the capacitance could plausibly be larger near the PZC, the constant capacitance estimates are upper bounds and the work function estimates are likely closer to the correct virtual PZC.

This work suggests possible areas for future study. UHV experiments and computation at higher levels of theory would help to more accurately determine the Cu-Cl system work function and identify possible functional errors in the HSE and PBE. Additionally, the full capacitance of the electrochemical interface is still unknown. We have modeled the Cu-Cl portion, but we do not know the capacitance contribution of the Cl-water portion of the interface. A related challenge is that we cannot eliminate the possibility that water may further lengthen the Cu-Cl interlayer spacing at experimentally relevant potentials, or that water at the interface would preferentially orient and drive the work function in a particular direction. More fully accounting for the water and electrolyte with *ab initio* molecular dynamics may improve these predictions. Simultaneously, experiments with nonaqueous solvents and cations larger than alkali metals could resolve the role of the electrolyte interactions on the interlayer spacing. Other solvents may also extend the experimentally accessible potential window, possibly to potentials where the Cu-Cl interlayer spacing, and hence, virtual PZC, would be expected to decrease. Finally, exploratory work could identify if the behavior of this Cl-covered surface is more general, extending to other interfaces with: 1) a PZC above the potential of interest and 2) adsorbates with a flexible bond and a dipole moment pointing in the direction of the electrolyte. Collectively these challenges present opportunity for future experiments, computations, and methods development.

Supporting Information

Additional computational details and convergence tests are contained in the supporting information, including pseudopotentials, plane-wave cut-off, k-point sampling and EXX downsampling, slab z-height and copper layers, single water calculation slab geometry, and work function change from vacuum to solvation model calculation.

References

- Schmickler, W. The surface dipole moment of species adsorbed from a solution. *J. Electroanal. Chem.* **1988**, *249*, 25–33.
- Schmickler, W. Electronic Effects in the Electric Double Layer. *Chem. Rev.* **1996**, *96*, 31773200.
- Trasatti, S. The absolute electrode potential: an explanatory note (Recommendations 1986). *Pure and Appl. Chem.* **58**.
- A. Spitzer,; Ritz, A.; H.Lüth, The adsorption of H_2O on Cu(100) surfaces. *Surf. Sci.* **1985**, *152–153*, 543–549.
- R.Brosseau,; M.R.Brustein,; T.H.Ellis, Water adsorption on Cu(100): The effect of defects. *Surf. Sci.* **1993**, *294*, 243–250.
- Puisto, M.; Pussi, K.; Alatalo, M.; Hesp, D.; Dhanak, V.; Lucas, C.; Grunder, Y. LEED – IV and DFT study of the co-adsorption of chlorine and water on Cu(100). *Surf. Sci.* **2017**, *657*, 51–57.
- Wang, L.-Q.; von Wittenau, A. E. S.; Ji, Z. G.; Wang, L. S.; Huang, Z. Q.; Shirley, D. A. $c(2 \times 2)Cl_1/Cu(001)$ adsorbate geometry and substrate-surface relaxation using low-temperature angle-resolved photoemission extended fine structure. *Phys. Rev. B* **44**, 1292–1305.
- Westphal, D.; Goldmann, A. Chlorine adsorption on copper: II. Photoemission from $Cu(001)c(2 \times 2)-Cl_1$ and $Cu(111)(\sqrt{3} \times \sqrt{3})R30^\circ$. *Surf. Sci.* **1983**, *131*, 113–138.
- Gartland, P.; Berge, S.; Slagsvold, B. Photoelectric Work Function of a Copper Single Crystal for the (100), (110), (111), and (112) Faces. *Phys. Rev. Lett.* **1972**, *28*, 738.
- Gründer, Y.; Lucas, C. A. Probing the charge distribution at the electrochemical interface. *Phys. Chem. Chem. Phys.* **2017**, *19*, 8416–8422.
- Groenenboom, M. C.; Moffat, T. P.; Schwarz, K. A. Halide-Induced Step Faceting and Dissolution Energetics from Atomistic Machine Learned Potentials on Cu(100). *J. Phys. Chem. C* **2020**, *124*, 12359–12369.
- Magnussen, O. M.; Groß, A. Toward an Atomic-Scale Understanding of Electrochemical Interface Structure and Dynamics. *J. Am. Chem. Soc.* **2019**, *141*, 47774790.
- Huemann, S.; Hai, N. T. M.; Broekmann, P.; Wandelt, K.; Zanjong, H.; Dosch, H.; Renner, F. X-ray Diffraction and STM Study of Reactive Surfaces under Electrochemical Control: Cl and I on Cu(100). *J. Phys. Chem. B* **2006**, *110*, 24955–24963.
- Vogt, M.; Lachenwitzer, A.; Magnussen, O.; Behm, R. In-situ STM study of the initial stages of corrosion of Cu(100) electrodes in sulfuric and hydrochloric acid solution. *Surf. Sci.* **1998**, *399*, 49–69.
- Gründer, Y.; Kaminski, D.; Golks, F.; Krug, K.; Stettner, J.; Magnussen, O. M.; Franke, A.; Stremme, J.; Pehlke, E. Reversal of chloride-induced Cu(001) subsurface buckling in the electrochemical environment: An in situ surface x-ray diffraction and density functional theory study. *Phys. Rev. B* **2010**, *81*, 174114.
- Lukomska, A.; Sobkowski, J. Potential of zero charge of monocrystalline copper electrodes in perchlorate solutions. *J. Electroanal. Chem.* **2004**, *567*, 95–102.
- Keller, H.; Saracino, M.; Nguyen, H.; Huynh, T.; Broekmann, P. Competitive Anion/Water and Cation/Water Interactions at Electrified Copper/Electrolyte Interfaces Probed by In Situ X-ray Diffraction. *J. Phys. Chem. C* **2012**, *116*, 1106811076.
- Keller, H.; Saracino, M.; Nguyen, H. M. T.; Broekmann, P. Templating the near-surface liquid electrolyte: In situ surface x-ray diffraction study on anion/cation interactions at electrified interfaces. *Phys. Rev. B* **2010**, *82*, 245425.
- Arjmand, F.; Adriaens, A. Influence of pH and Chloride Concentration on the Corrosion Behavior of Unalloyed Copper in NaCl Solution: A Comparative Study Between the Micro and Macro Scales. *Materials* **2012**, *5*, 2439–2464.
- G.Kear,; B.D.Barker,; F.C.Walsh, Electrochemical corrosion of unalloyed copper in chloride media—a critical review. *Corros. Sci.* **2004**, *46*, 109–135.
- Saracino, M.; Broekmann, P.; Gentz, K.; Becker, M.; Keller, H.; Janetzko, F.; Bredow, T.; Wandelt, K.; Dosch, H. Surface relaxation phenomena at electrified interfaces: Revealing adsorbate, potential, and solvent effects by combined x-ray diffraction, STM and DFT studies. *Phys. Rev. B* **2009**, *79*, 115448.
- Migani, A.; Illas, F. A Systematic Study of the Structure and Bonding of Halogens on Low-Index Transition Metal Surfaces. *J. Phys. Chem. B* **2006**, *110*, 11894–11906.
- Roman, T.; Groß, A. Periodic Density-Functional Calculations on Work-Function Change Induced by Adsorption of Halogens on Cu(111). *Phys. Rev. Lett.* **110**, 156804.
- G.Liu,; Zou, S.; Josell, D.; Richter, L.; Moffat, T. SEIRAS Study of Chloride Mediated Polyether Adsorption on Cu. *J. Phys. Chem. C* **2018**, *122*, 21933–21951.
- C.Figueiredo, M.; Hiltrop, D.; Sundararaman, R.;

- A.Schwarz, K.; T.M.Koper, M. Absence of diffuse double layer effect on the vibrational properties and oxidation of chemisorbed carbon monoxide on a Pt(111) electrode. *Electrochim. Acta* **2018**, *281*, 127 – 132.
- (26) Sundararaman, R.; Figueiredo, M. C.; Koper, M.; Schwarz, K. A. Electrochemical capacitance of CO-terminated Pt (111) is dominated by CO-solvent gap. *J. Phys. Chem. Lett.* **2017**, *8*, 5344–5348.
- (27) Le, J.; Iannuzzi, M.; Cuesta, A.; Cheng, J. Determining Potentials of Zero Charge of Metal Electrodes versus the Standard Hydrogen Electrode from Density-Functional-Theory-Based Molecular Dynamics. *Phys. Rev. Lett.* **2017**, *119*, 016801.
- (28) Schnur, S.; Groß, A. Properties of metal–water interfaces studied from first principles. *New J. Phys.* **2009**, *11*.
- (29) K.Bange.; Döhl, R.; Grider, D. E.; Sass, J. K. Water adsorption on bromine-covered copper single crystal surfaces. *Vacuum* **1983**, *33*, 757–761.
- (30) Tolentino, H. C. N.; Santis, M. D.; Gauthier, Y.; ; Langlais, V. Chlorine chemisorption on Cu(001) by surface X-ray diffraction: Geometry and substrate relaxation. *Surf. Sci.* **2007**, *601*, 2962.
- (31) Perdew, J. P.; Burke, K.; Ernzerhof, M. Generalized Gradient Approximation Made Simple. *Phys. Rev. Lett.* **1996**, *77*, 3865–3868.
- (32) (a) Heyd, J.; Scuseria, G. E.; Ernzerhof, M. Hybrid functionals based on a screened Coulomb potential. *J. Chem. Phys.* **2003**, *118*, 8207–8215; (b) Heyd, J.; Scuseria, G. E.; Ernzerhof, M. Erratum: “Hybrid functionals based on a screened Coulomb potential” [J. Chem. Phys. 118, 8207 (2003)]. *J. Chem. Phys.* **2006**, *124*, 219906.
- (33) van Setten, M.; Giantomassi, M.; Bousquet, E.; Verstraete, M.; Hamann, D.; Gonze, X.; Rignanese, G.-M. The PseudoDojo: Training and grading a 85 element optimized norm-conserving pseudopotential table. *Computer Physics Communications* **2018**, *226*, 39 – 54, PBE-PDv0.4; Cl-sp, Cu-sp-high.
- (34) Giannozzi, P.; Basergio, O.; Bonfà, P.; Brunato, D.; Car, R.; Carnimeo, I.; Cavazzoni, C.; de Gironcoli, S.; Delugas, P.; Ferrari Ruffino, F.; Ferretti, A.; Marzari, N.; Timrov, I.; Urru, A.; Baroni, S. Quantum ESPRESSO toward the exascale. *J. Chem. Phys.* **2020**, *152*, 154105.
- (35) Lin, L. Adaptively Compressed Exchange Operator. *J. Chem. Theory Comput.* **2016**, *12*, 2242–2249.
- (36) Vinson, J. Faster exact exchange in periodic systems using single-precision arithmetic. *J. Chem. Phys.* **2020**, *153*, 204106.
- (37) Yu, M.; Trinkle, D. Accurate and efficient algorithm for Bader charge integration. *J. Chem. Phys.* **2011**, *134*, 064111.
- (38) Bader, R. A quantum-theory of molecular-structure and its applications. *Chem. Rev.* **1991**, *91*, 893–928.
- (39) Bader, R. In *Atoms in Molecules. A Quantum Theory*; Oxford University Press, O., Ed.; 1990.
- (40) de-la Roza, A. O.; Johnson, E. R.; Luaña, V. Critic2: A program for real-space analysis of quantum chemical interactions in solids. *Comp. Phys. Comm.* **2014**, *185*, 1007–1018.
- (41) de-la Roza, A. O.; Blanco, M.; A. Martín Pendás, V. L. Critic: a new program for the topological analysis of solid-state electron densities. *Comp. Phys. Comm.* **2009**, *180*, 157–166.
- (42) Sundararaman, R.; Letchworth-Weaver, K.; Schwarz, K. A.; Gunceler, D.; Ozhabes, Y.; Arias, T. JDFTx: Software for joint density-functional theory. *SoftwareX* **2017**, *6*, 278 – 284.
- (43) Sundararaman, R.; Goddard, W. The Charge-Asymmetric Nonlocally-Determined Local-Electric (CANDLE) Solvation Model. *J. Chem. Phys.* **2015**, *142*, 064107.
- (44) Gunceler, D.; Letchworth-Weaver, K.; Sundararaman, R.; Schwarz, K.; Arias, T. The importance of nonlinear fluid response in joint density-functional theory studies of battery systems. *Model. Simul. Mater. Sci. Eng.* **2013**, *21*, 074005.
- (45) Schwarz, K.; Sundararaman, R. The electrochemical interface in first-principles calculations. *Surf. Sci. Rep.* **2020**, *75*, 100492.
- (46) Otani, M.; Sugino, O. First-principles calculations of charged surfaces and interfaces: A plane-wave nonrepeated slab approach. *Phys. Rev. B* **2006**, *73*, 115407.
- (47) Trasatti, S. Work function, electronegativity, and electrochemical behaviour of metals: II. Potentials of zero charge and “electrochemical” work functions. *J. Electroanal. Chem. Interfacial Electrochem.* **1971**, *33*, 351–378.
- (48) Tang, Q.-L.; Chen, Z.-X. Density functional slab model studies of water adsorption on flat and stepped Cu surfaces. *Surf. Sci.* **2007**, *601*, 954–964.
- (49) Otani, M.; Sugino, O. First-principles calculations of charged surfaces and interfaces: A plane-wave nonrepeated slab approach. *Phys. Rev. B* **2006**, *73*, 115407.
- (50) Peljhan, S.; Kokalj, A. Adsorption of Chlorine on Cu(111): A Density-Functional Theory Study. *J. Phys. Chem. C* **2009**, *113*, 14363–14376.
- (51) Suleiman, I. A.; Radny, M. W.; Gladys, M. J.; Smith, P. V.; Mackie, J. C.; Kennedy, E. M.; Dlugogorski, B. Z. Chlorination of the Cu(110) Surface and Copper Nanoparticles: A Density Functional Theory Study. *J. Phys. Chem. C* **2011**, *115*, 13412–13419.
- (52) Pavlova, T. V.; Andryushechkin, B. V.; Zhidomirov, G. M. First-Principle Study of Adsorption and Desorption of Chlorine on Cu(111) Surface: Does Chlorine or Copper Chloride Desorb? *J. Phys. Chem. C* **2016**, *120*, 2829–2836.
- (53) Feibelman, P. J.; Hammer, B.; Norskov, J. K.; Wagner, F.; Scheffler, M.; Stumpf, R.; Watwe, R.; Dumesic, J. The CO/Pt(111) Puzzle. *J. Phys. Chem. B* **2001**, *105*, 4018–4025.
- (54) Nilius, N.; Fedderwitz, H.; Groß, B.; Noguera, C.; Goniakowski, J. Incorrect DFT-GGA predictions of the stability of non-stoichiometric/polar dielectric surfaces: the case of Cu₂O(111). *Phys. Chem. Chem. Phys.* **2016**, *18*, 6729–6733.
- (55) Liu, W.; Tkatchenko, A.; ; Scheffler, M. Modeling Adsorption and Reactions of Organic Molecules at Metal Surfaces. *Acc. Chem. Res.* **2014**, *47*, 3369–3377.
- (56) Lage-Estebanez, I.; Ruzanov, A.; de la Vega, J. M. G.; Fedorov, M. V.; Ivaništšev, V. B. Self-interaction error in DFT-based modelling of ionic liquids. *Phys. Chem. Chem. Phys.* **2016**, *18*, 2175–218.

Resolving the Geometry/Charge Puzzle of the c(2x2)-Cl Cu(100) Electrode

Kathleen Schwarz,^{*,†} Mitchell C. Groenenboom,[†] Thomas P. Moffat,[†]
Ravishankar Sundararaman,[‡] and John Vinson[†]

[†]*Material Measurement Laboratory, National Institute of Standards and Technology, 100
Bureau Dr., Gaithersburg, Maryland 20899, United States*

[‡]*Department of Materials Science and Engineering, Rensselaer Polytechnic Institute, 110
8th St., Troy, New York 12180, United States*

E-mail: kas4@nist.gov

Pseudopotentials

The pseudopotential input files were taken from the PseudoDojo library, PBE v0.4. The inputs were modified to remove the non-local core corrections. The pseudopotentials were created using a modified version of the oncvpsp.x code (v3.3.1). The matching radius for inward and outward integration of the partial waves was changed from 10 times the classical turning radius to 20 times. This change was to avoid numerical noise at medium distances in the local potential. As shown in Fig 1, the local potential of Cu from the unmodified oncvpsp.x code deviates from the expected $-Z/r$ behavior (here Z is the pseudopotential charge 19). This modification was made because within QuantumESPRESSO the correct behavior is enforced starting at 10 a.u. (5.3 Å), but within jDFTx no correction is applied.

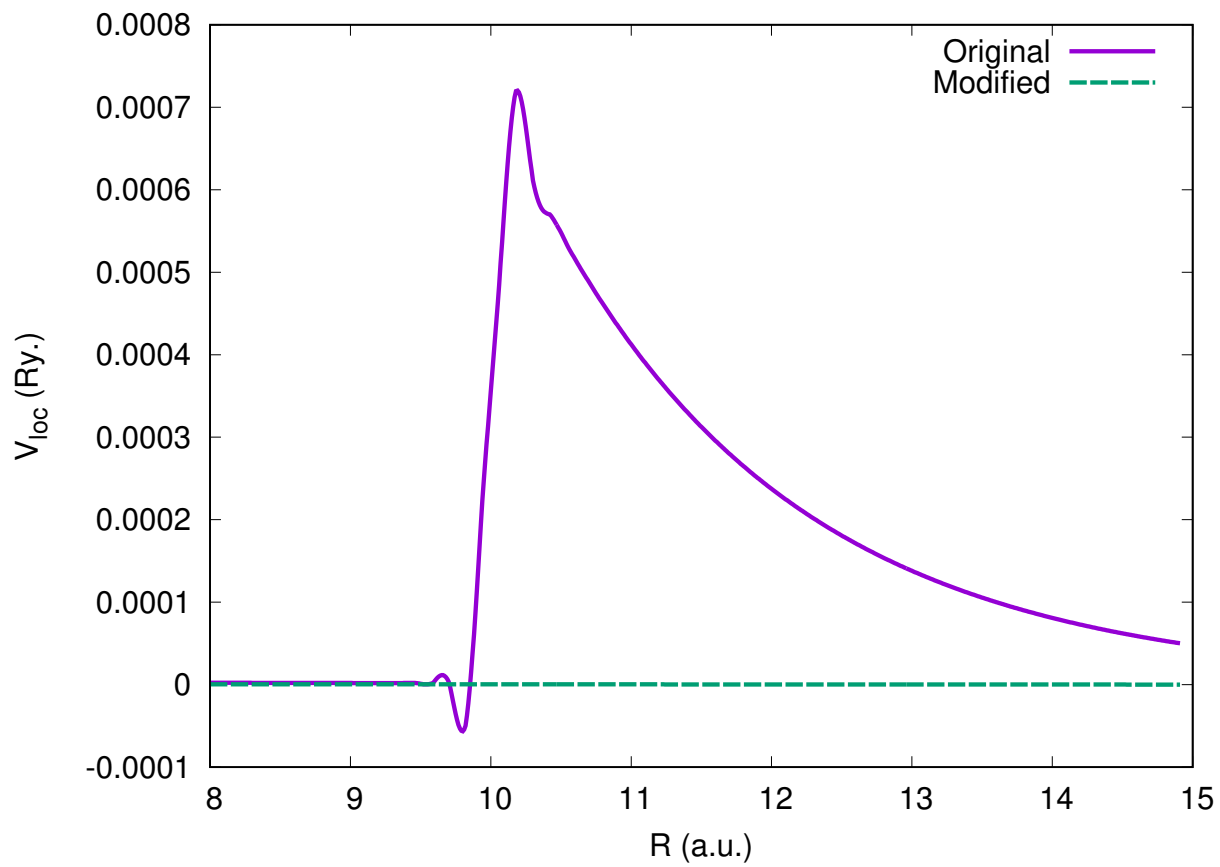


Figure 1: The deviation local potentials from the original and modified copper pseudopotentials from the expected $-Z/r$ behavior.

QuantumESPRESSO calculations

Plane-wave cut-off

Using the PBE functional we checked convergence of the planewave energy cut-off using bulk copper and CuCl (cubic CuCl-V). A cut-off energy of 120 Ry (1630 eV) was found to be sufficient to converge the total energy per atom to better than 0.002 eV/atom.

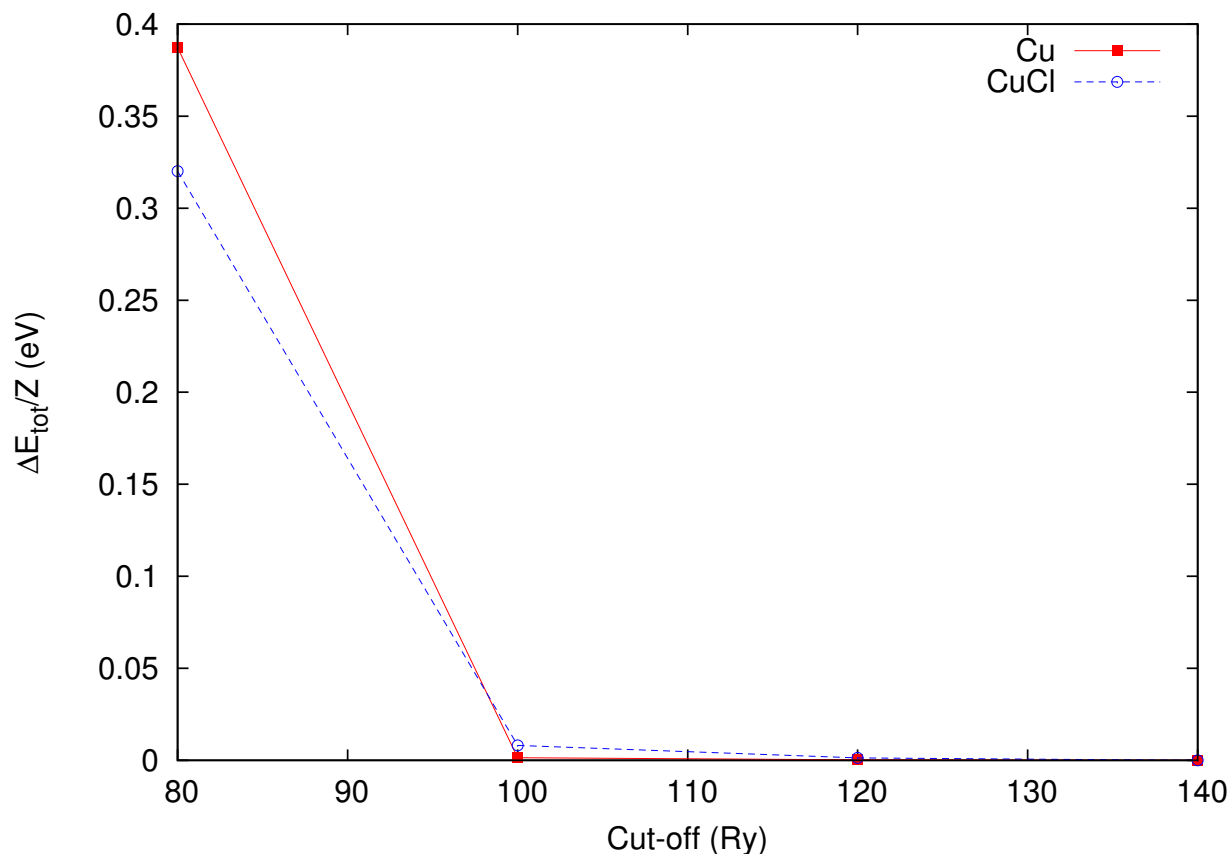


Figure 2: The deviation local potentials from the original and modified copper pseudopotentials from the expected $-Z/r$ behavior.

K-point sampling and EXX downsampling

The calculation of the exact exchange can be carried out using a reduced q-point mesh, subject to the constraint that the q-point mesh is an integer factor of the k-point mesh. Using bulk Cu, the energy as a function of volume was calculated for 9 equally spaced lattice

vectors from 6.70 a.u. (3.55 Å) to 7.02 a.u. (3.71 Å). These calculations were carried out on a 10^3 shifted k-point mesh with 10^3 q-point sampling of the exact exchange. They were then repeated for a 10^3 k-point mesh with 5^3 downsampling and 8^3 k-point with both 8^3 and 4^3 downsampling. For each, the equation of state was calculated using the 3rd order Birch–Murnaghan equation, allowing a comparison of the equilibrium lattice constant and the bulk modulus. Across these calculations the equilibrium lattice constant differed from the initial run by less than 0.05.

For the slab calculations (20 Cu and 2 Cl) an $8 \times 8 \times 1$ k-point sampling and $4 \times 4 \times 1$ q-point downsampling was used. The x and y lattice vector lengths for the unit cells of the slab are $\sqrt{2}$ larger than the bulk Cu primitive cell, making the effective k-point density slightly larger than the 10^3 grid.

Z-height and copper layers

To converge the z-height of the cell, PBE calculations were carried out on a slab (20 Cu and 2 Cl), using 6.85 a.u. (3.62 Å) for the x and y dimensions and varying the z dimension. Along z, vacuum boundary conditions were enforced via the ESM. The atoms were allowed to relax until the forces were below a threshold of 10^{-5} Ry/a.u. The convergence with respect to simulation height is shown in Table 3, and the convergence with respect to the number of copper atoms is shown in Table 4.

Z (a.u.) [Å]	E_{Fermi} (eV)	d_{Cu-Cl} (Å)	Δ_2 (Å)
60 [31.8]	-5.282	1.6595	0.0036
70 [37.0]	-5.285	1.6608	0.0060
80 [42.3]	-5.284	1.6604	0.0054
90 [47.6]	-5.281	1.6596	0.0063

Figure 3: Convergence of the Fermi level, Cu-Cl spacing and, buckling (Δ_2) with simulation cell height Z using 20 copper atoms.

N_{Cu}	E_{Fermi} (eV)	d_{Cu-Cl} (Å)	Δ_2 (Å)
20	-5.284	1.6604	0.0054
24	-5.305	1.6606	0.0039
28	-5.294	1.6606	0.0039

Figure 4: Convergence of the Fermi level, Cu-Cl spacing and, buckling (Δ_2) with the number of copper atoms using a simulation cell of height $Z=80$ a.u.

Production runs

As noted the runs were carried out on unit cells (20 Cu and 2 Cl), $6.85 \times 6.85 \times 60$ a.u. ($3.62 \text{ \AA} \times 3.62 \text{ \AA} \times 31.8 \text{ \AA}$). The plane-wave cut-off was set to 120 Ry (1630 eV) and an $8 \times 8 \times 1$ k-point grid (shifted by $1/16, 1/16, 0$) was used. From the results above, these settings give the Fermi level to better than 0.02 eV and relative atomic positions to within 0.002 Å. For the charged calculations, the atoms were allowed to relax until their forces were below a threshold of 10^{-4} Ry/a.u. (2.5×10^{-3} eV/Å). The atom positions were fixed for the “stretch” calculations. First, the atomic coordinates were taken from the relaxed positions of the uncharged system, and then Cl atoms were moved symmetrically out from the Cu slab. Charged calculations in excess of $0.1 e^-/Cl$ accumulated charge at the boundary, an effect which persisted for a larger $z=80$ a.u. (42.3 \AA) cell as well.

Single-water calculations

Figure 5 depicts the geometry of a single-water calculations under $0.35 e^-/Cl$.

Work function change from vacuum to solvation model

The work function for the $c(2 \times 2)$ Cl-covered Cu(100) surface in the presence of CANDLE solvation is lower than the vacuum value by 0.16 V. This small shift reflects the parameterization of the solvation model and the hydrophobicity of the surface.

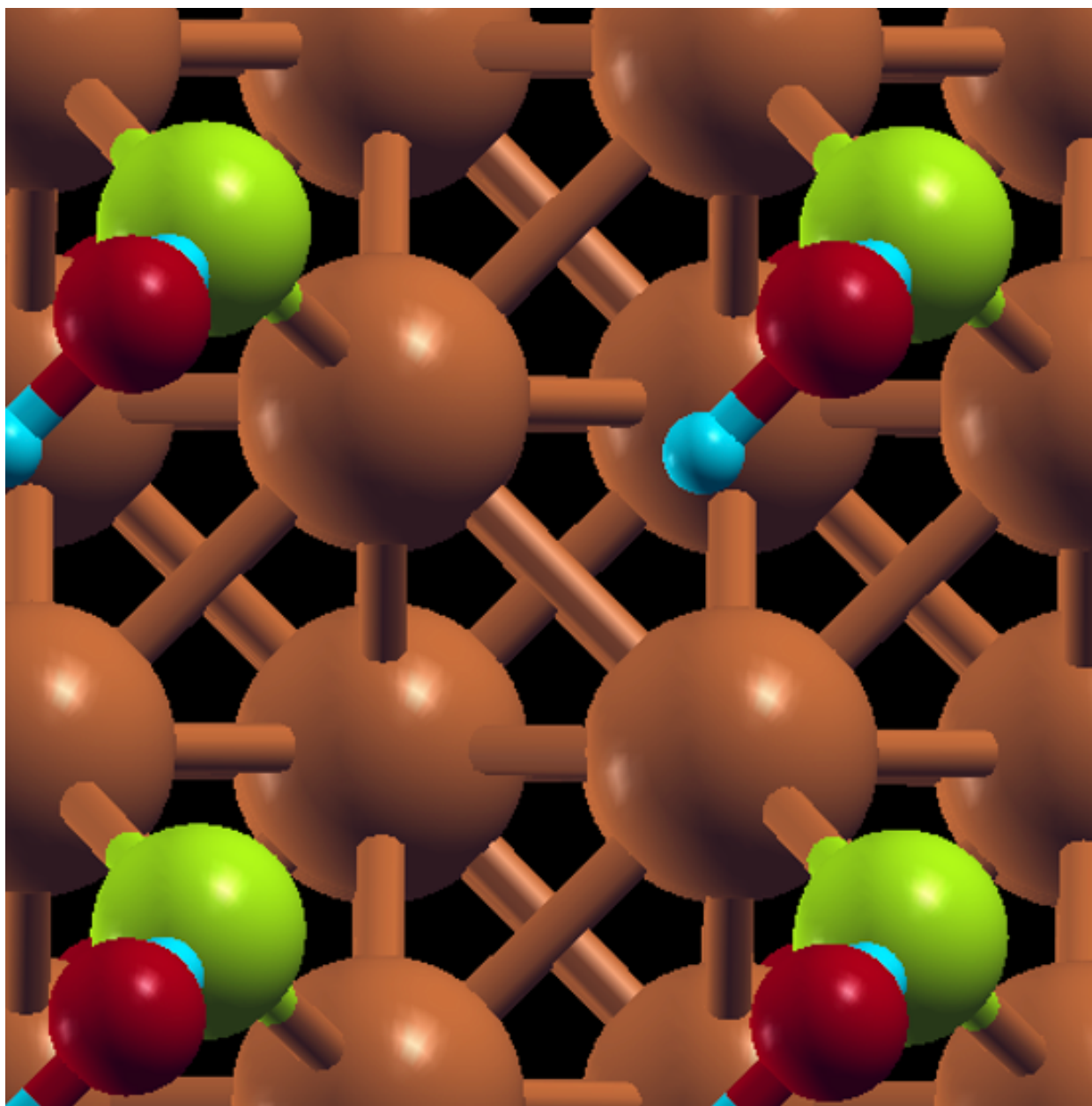


Figure 5: Calculation with $0.35 e^-/\text{Cl}$ and a single water molecule, illustrating the (unphysical) geometry of the Cl at a bridge site instead of the experimentally observed hollow site. HSE calculations at these higher charges are necessary to check if this is a self-interaction or other DFT error.